Title

Clinical and imaging characteristics of late onset mitochondrial membrane protein-associated neurodegeneration (MPAN)

Journal

Neurocase, 22(5)

ISSN

1355-4794

Authors

Gore, Ethan
Appleby, Brian S
Cohen, Mark L
et al.

Publication Date

2016-09-02

DOI

10.1080/13554794.2016.1247458

Peer reviewed

Published in final edited form as:

Neurocase. 2016 October ; 22(5): 476–483. doi:10.1080/13554794.2016.1247458.

Clinical and imaging characteristics of late onset mitochondrial membrane protein-associated neurodegeneration (MPAN)

Ethan Gore[a], **Brian S. Appleby**[b], **Mark L. Cohen**[c], **Suzanne D. DeBrosse**[d], **James B. Leverenz**[e], **Bruce L. Miller**[f], **Sandra L. Siedlak**[g], **Xiongwei Zhu**[g], and **Alan J. Lerner**[a]

[a]Department of Neurology, University Hospitals Case Medical Center, Beachwood, OH, USA

[b]Departments of Neurology and Psychiatry, University Hospitals Case Medical Center, 3619 Park East Drive, Beachwood, OH, USA

[c]Department of Pathology, University Hospitals Case Medical Center, Cleveland, OH, USA

[d]Departments of Genetics and Genome Sciences, Pediatrics, and Neurology, University Hospitals Case Medical Center, Cleveland, OH, USA

[e]Cleveland Clinic Lou Ruvo Center for Brain Health, Cleveland, OH, USA

[f]Department of Neurology, University of California, San Francisco, San Francisco, CA, USA

[g]Department of Pathology, Case Western Reserve University, Cleveland, OH, USA

Abstract

Young onset dementias present significant diagnostic challenges. We present the case of a 35-year-old Kuwaiti man with social withdrawal, drowsiness, irritability, anxiety, aphasia, memory loss, hypereflexia, and Parkinsonism. Brain MRI showed bilateral symmetric gradient echo hypointensities in the globi pallidi and substantiae nigrae. Left cortical hypometabolism was seen on brain fluorodeoxyglucose positron emission tomography. A cortical brain biopsy revealed a high Lewy body burden. Genetic testing revealed a homozygous p.T11M mutation in the C19orf12 gene consistent with mitochondrial membrane protein-associated neurodegeneration. This is the oldest onset age of MPAN reported.

Keywords

Mitochondrial membrane; protein-associated; neurodegeneration (MPAN); neurodegeneration with brain iron accumulation (NBIA); Lewy body; Parkinsonism; whole exome sequencing

Introduction

Recent advances in imaging and genomic analysis have allowed the definitive diagnosis of hereditary causes of dementia prior to autopsy. We present the case of a young man, born to consanguineous parents, who developed dementia with pyramidal and extrapyramidal signs

CONTACT: Ethan Gore, ethanmgore@gmail.com.

Disclosure statement

The authors have no financial or nonfinancial relationships to disclose.

associated with symmetric gradient echo (GRE) hypointensities of the globi pallidi on magnetic resonance imaging (MRI). Whole exome sequencing revealed a homozygous mutation in C19orf12 causing the oldest known onset of mitochondrial membrane protein associated neurodegeneration (MPAN). Like the other two MPAN pathology reports, this patient's brain biopsy revealed a high Lewy body burden. In this paper, we review the clinical, genetic, and histological characteristics of MPAN.

Case

A 35-year-old Kuwaiti police officer presented to a clinic in Kuwait for a change in behavior in early 2014. Over the prior 2 months, he had developed "nonsense talking" characterized by semantic paraphasias with preserved fluency, blunted affect, social withdrawal, memory problems, and drowsiness. He complained of a new mild tremor in his hands when nervous. There was no history of head trauma. His parents were consanguineous (see Figure 1). Three of his six siblings had intellectual disability and dysmorphic features. Exam at that time showed an Arabic Mini Mental Status Exam score of 23/30, and the remainder of the exam was normal except for mild hypereflexia.

His Vitamin B12 level was 185 ng/L (abnormal < 150 ng/L). The following laboratory studies were unremarkable: comprehensive metabolic panel, thyroid-stimulating hormone, erythrocyte sedimentation rate, antinuclear antibody, C-reactive protein, urinalysis, ammonia, copper, ceruloplasmin, heavy metals, coagulation studies, anti-thyroglobulin antibody, antithyroperoxidase antibody, paraneoplastic panel, serum lactate, and plasma amino acids. His routine CSF studies were normal, and there were no oligoclonal bands. MRI of the brain is shown in Figure 2. Fluorodeoxyglucose positron emission tomography (FDG-PET) showed hypometabolism in left parietal, temporal, anterior occipital, and left caudate nucleus (see Figure 3). A left frontal cortical brain biopsy performed to rule out vasculitis showed no evidence of vasculitis but did reveal many intracytoplasmic neuronal spheroids and a few similar appearing extraneuronal spheroids. These inclusions were labeled by p62 and alpha-synuclein immunohistochemistry stains confirming their identity as Lewy bodies. The biopsied tissue from the dura mater, leptomeninges, and subcortex was normal (see Figure 4). CT of the brain after the biopsy is shown in Figure 5.

Eleven months after onset, his speech had gradually worsened so that he could only speak a few words, and he had developed slow movement, imbalance, festination, acalculia, poor memory, anxiety, and irritability. He was sleeping up to 14 h/day. On examination, he was well dressed and nourished with good eye contact. His mood was described as "Okay," and his affect was full range. His Arabic Montreal Cognitive Assessment score was 8/30 demonstrating a predominantly receptive aphasia with relatively preserved repetition. He had no spontaneous speech, and his verbal responses were brief. He had clonus of the ankles, brisk deep tendon reflexes, and a positive glabellar sign. He had bradykinesia and decreased arm swing worse on the left side and a mild bilateral resting tremor.

Genetic testing was performed, and whole exome sequencing at GeneDx laboratory (Gaithersburg, MD) revealed a homozygous p.T11M mutation in C19orf12 consistent with

mitochondrial MPAN, a form of neurodegeneration with brain iron accumulation (NBIA) (Accession numbers: NM_001031726.2 and NM_031448.3).

Deferiprone, an iron chelator, was experimentally prescribed but not tolerated due to gastrointestinal side effects (Aoun & Tiranti, 2015; Cossu et al., 2014). Over his second year of illness, the patient developed frequent visual hallucinations, rapid eye movement sleep behavior disorder, urinary and bowel incontinence, staring spells lasting up to 15 min, inappropriate laughter and crying, and apraxia. As of March 2016, he was able to walk without assistance, but he needed help preparing meals and around the clock supervision due to frequent wandering.

Discussion

The first symptoms of this patient's neurological disorder were tremor, slow gait, social withdrawal, transcortical sensory aphasia, poor concentration, and drowsiness. This constellation of symptoms raises concern for a bilateral cortical, subcortical, basal ganglia, thalamic, and upper brainstem dysfunction worse on the left side. The differential diagnosis for such a presentation is broad and includes Wilson's disease, Huntington's disease, Huntington's disease-like 2, young onset Parkinson's disease, neuroacanthocytosis, and other NBIAs (see Table 1) (Freeman et al., 2007; Gregory & Hayflick, 2014; Gregory et al., 2008; Hayflick, 2014; Karkheiran, Shahidi, Walker, & Paisan-Ruiz, 2015; Keogh, Jonas, Coulthard, Chinnery, & Burn, 2012; Kurian & Hayflick, 2013; Lehn, Boyle, Brown, Airey, & Mellick, 2012; Levine, Estes, & Looney, 1968; Mahoney, Selway, & Lin, 2011; Margolis et al., 2001; Margolis, 2012; McNeill, Pandolfo, Kuhn, Shang, & Miyajima, 2008; Schneider & Bhatia, 2012; Schneider & Bhatia, 2012; Schrag, Ben-Shlomo, Brown, Marsden, & Quinn, 1998; Stevenson & Hardie, 2001; Williams, Hadeed, al-Din, Wreikat, & Lees, 2005; Yonekawa, Okabe, Asamoto, & Ohta, 1999).

NBIA is a group of disorders caused by mutations in 10 known genes (Gregory & Hayflick, 2014). The prevalence of NBIA is less than one per million people in the United States. The most common NBIA disorders are pantothenate kinase-associated neurodegeneration (PKAN) due to mutations in pantothenate kinase 2 (PANK2) followed by phospholipase A2 group VI (PLA2G6)-associated neurodegeneration (PLAN) due to mutations in PLA2G6 which together comprise over half the cases. The third most common NBIA disorder is mitochondrial MPAN which is caused by mutations in C19orf12 and accounts for 5–30% of NBIA cases (Gagliardi et al., 2015; Hartig, Prokisch, Meitinger, & Klopstock, 2013; Hogarth et al., 2013). A C19orf12 mutation associated with brain iron accumulation was first described in 2011 in three members of a Polish family who had NBIA but no PANK2 mutation. Targeted genetic sequencing of 23 other Polish NBIA patients without PANK2 mutations revealed C19orf12 mutations in 11 of them (Hartig et al., 2011). To date, fewer than 100 cases of MPAN have been described.

MPAN is an autosomal recessively inherited disease caused by mutations in C19orf12, which encodes a protein of unknown function found throughout the body, especially expressed in the brain, blood cells, and adipocytes (Colombelli, Aoun, & Tiranti, 2015). The protein has been localized to mitochondria, endoplasmic reticula, and mitochondrial-

associated membranes, and its long hydrophobic domain and glycine zipper motifs suggest that it may be a transmembrane protein (Venco et al., 2015). Mutations in C19orf12 result in a higher percentage of the protein outside the mitochondria perhaps due to inability to fit into membranes. The gene is co-regulated with genes involved in fatty acid biogenesis and in degradation of branched chain amino acids. These processes are both related to coenzyme A metabolism which is dysfunctional in other types of NBIA (Levi & Finazzi, 2014; Meyer, Kurian, & Hayflick, 2015)). In contrast to the better understood pathophysiologies of aceruloplasminemia and neuroferritinopathy, it is unclear specifically why brain iron accumulation and brain dysfunction occur in people with MPAN.

The mean age at onset of MPAN is 10 years of age, and cases have been reported between 3 and 30 years of age (Gregory et al., 2014). Usually, the first signs are gait changes that progress to spastic paraparesis and dystonia which may be limited to the hands and feet. In seven patients reported, the average age of wheelchair requirement was 21.7 years of age (Hartig et al., 2013).

This patient's disease broadens the spectrum of MPAN as it is the oldest onset of the disease at 35 years of age. Other p. T11M C19orf12 mutations have also been associated with older than average onset (Dezfouli et al., 2013). The T11M mutation is a missense mutation that has been reported in at least eight families. C19orf12 encodes a long and a short isoform that differ by 11 amino acids based on 2 alternative first exons. The vast majority of the C19orf12 mutations affect both isoforms. The T11M mutation only affects the long isoform which implicates its involvement in the pathogenesis of MPAN. In six patients from five families with homozygous p. T11M mutations, the average onset age was 25 years of age, ranging from 21 to 28. Chimpanzees and chickens are the only other known species with two isoforms of C19orf12, raising the possibility of an animal model of MPAN. Other species evaluated only have a short isoform.

Neuropsychiatric symptoms are common at onset and include labile mood, depression, anxiety, hallucinations, perseveration, inattention, and hyperactivity. In children, it may present as attention deficit hyperactivity disorder congener. Dysarthria from oromandibular dystonia is very common and often presents early in the disease. Dysphagia occurs in about half of people with MPAN. Parkinsonism is seen in about half of cases, and its response to dopaminergic agents is variable and without dyskinesia. Optic atrophy is reported in over 70% of MPAN patients and is more prominent in young onset cases, whereas Parkinsonism is more prominent with older onset (Kleffner et al., 2015). Four of 23 patients with MPAN first sought medical care due to vision loss related to optic atrophy.

Two clinical symptoms distinguishing MPAN from other NBIA disorders are early incontinence and motor axonal polyneuropathy. Eleven of 17 people with C19orf12 mutations developed urinary incontinence, often prior to severe walking or cognitive problems. Nine of 13 MPAN patients who underwent electrophysiological testing showed evidence of motor axonal neuropathy which can be severe. MPAN patients with a positive Babinski sign and hyporeflexia and distal atrophy have been described (Deschauer et al., 2012; Dogu et al., 2013). Skin biopsy in two MPAN patients revealed axonal spheroids. This patient developed incontinence within 2 years and early in the clinical course had

hypereflexia. He did not undergo a nerve conduction study. MPAN progresses over 1 year to a few decades, nearly universally causes dementia, and is uniformly fatal. There are no specific treatments; a few clinical trials have used iron chelators in patients with NBIA but no patients with MPAN were included (Cossu et al., 2014; Zorzi et al., 2011).

Lactate dehydrogenase may be high in MPAN, but otherwise routine laboratory testing is unremarkable (Schulte et al., 2013). Brain MRI in MPAN typically shows T2 hypointensity of the globi pallidi and substantiae nigrae with generalized atrophy that depends on the stage of the illness. The T2 hypointensity is due to susceptibility effects related to increased paramagnetic iron accumulation and is, therefore, seen best using susceptibility weighted sequences like GRE. On T2-weighted images, some MPAN patients have hyperintense streaking that highlights the entire length of the medullary lamina between the internal and external segments of the globus pallidus (Amaral et al., 2015). This streaking may occur due to inflammation, or simply sparing from iron accumulation. This may appear similar to the “eye of the tiger” sign usually seen in PKAN as a rounded, drop-like T2 hyperintensity at the anterior end of the medullary lamina over a background of hypointense globi pallidi (Hayflick, Hartman, Coryell, Gitschier, & Rowley, 2006; Skowronska, Kmiec, Kurkowska-Jastrzębska, & Czlonkowska, 2015).

Prior research is unclear about when brain iron accumulation occurs and whether or not increased brain iron accumulation always eventually occurs with C19orf12 mutations. Two Malian sisters, ages 7 and 12, developed progressive spastic paraparesis and peripheral neuropathy and were found to have C19orf12 mutations but no extrapyramidal symptoms, cognitive deficits, or optic atrophy even 5 years later. In 2010, before the first description of MPAN, their syndrome was called hereditary spastic paraplegia type 43 (Landoure et al., 2013). A brain MRI in one of the siblings showed no basal ganglia hypointensity. Two Brazilian siblings, ages 14 and 15, with the same genotype who also presented with progressive spastic paraparesis were found to have iron deposition on MRI and optic atrophy, and one had cognitive deficits, but neither had extrapyramidal symptoms. Observation and analysis of these cases may provide insight into how brain damage occurs in MPAN.

No standardized formula exists to distinguish between physiologic and pathologic brain iron accumulation. Brain iron increases with age, and T2 hypointensity from iron becomes more prominent with increasing magnetic field strength (Aoki et al., 1989; Schenck, 1995; Schneider et al., 2013). In a young symptomatic patient with basal ganglia hypointensities on T2 and especially SWI, we felt that NBIA-genetic testing was appropriate (International Huntington Association and the World Federation of Neurology Research Group on Huntington’s Chorea, 1994; Points to Consider in the Clinical Application; Rabbani, Tekin, & Mahdieh, 2014).

In MPAN, the globus pallidus usually appears normal or sometimes slightly hyperintense on T1 images. This may be due to an iron-related discrepancy between the paramagnetic effect on T1 and T2 shortening as has been described with manganese. In our patient’s case, the globus pallidus was hypointense on T1 images, which is unreported. Because the globus pallidus in this case appears hypointense on T2 and SWI sequences as expected, we believe

that the globus pallidus T1 hypointensity is due to iron-related susceptibility artifact that is stronger with a 3T magnet than the prior brain MRIs of patients with MPAN obtained with 1.5T magnets. Brain iron deposition can cause a uniform T1 hypointensity less prominent than that on T2 (Hegde, Mohan, Lath, & Lim, 2011; del C. Valdés Hernández et al., 2014; del C. Valdés Hernández, Maconick, Tan, & Wardlaw, 2012).

Another feature of this MRI that is atypical in MPAN is the hypointensity of the caudate and putamen on FLAIR and SWI. Hypointensity of the dorsal striatum has been reported in MPAN but not to the degree seen here (Dogu et al., 2013; Goldman et al., 2013; Hartig et al., 2013). Because the striatal-imaging characteristics are similar to those in the globus pallidus, we believe the striatal signal changes are due to iron deposition. Histological evidence of elevated iron in the caudate and putamen specifically in MPAN has not been reported. The hypointensities may appear more dramatic in this case due to a higher magnetic field strength or due to greater iron deposition. Striatal involvement has been shown in other patients with homozygous T11M mutations and in a younger patient with a different mutation (Dogu et al., 2013; Goldman et al., 2013; Hartig et al., 2013). Based on the small number of cases with caudate and putamen changes, we do not believe the presence or degree of MRI hypointensity of the caudate and putamen to be predictive of a particular MPAN mutation type.

This patient’s MRI shows a higher degree of asymmetric parenchymal volume loss than other reported MRIs in MPAN. It is corroborated by asymmetric metabolism on FDG-PET imaging. Our case is the first to report FDG-PET in MPAN, and it is unknown whether or not metabolic asymmetry should be considered typical of MPAN. The cortical hypometabolism shown in Figure 3 correlates well with this patient’s clinical presentation, but surprisingly the basal ganglia metabolism was relatively spared.

Microscopic examination of two MPAN brains revealed iron in the basal ganglia, especially the globus pallidus, with iron deposition in neurons, astrocytes, and perivascular macrophages. In those cases, extremely high concentrations of Lewy bodies were found in the cortex, hippocampus, brainstem, spinal cord, and basal ganglia, especially the globus pallidus. In the substantia nigra, Lewy bodies and Lewy neurites were accompanied by nearly complete axonal loss. Axonal spheroids and hyperphosphorylated tau-containing inclusions were also seen in the brain. Ultrastructural studies of the Lewy bodies are ongoing but beyond the scope of this paper.

The biopsy in this case is the third reported histological examination of brain tissue from a patient with MPAN. Like the other two, it revealed very high concentrations of cortical Lewy bodies. Similar to other patients with alpha-synucleinopathies, this patient developed frequent well-formed visual hallucinations, staring spells lasting up to 15 min, rapid eye movement sleep behavior disorder, and incontinence. Although the cause of alpha-synucleinopathies remains unclear, growing evidence implicates mitochondrial dysfunction. With more confidence that MPAN is an alpha-synucleinopathy, the already established link between alpha-synucleinopathies and mitochondrial dysfunction becomes stronger. Thinking of MPAN as an alpha-synucleinopathy may help to untangle the complex association between the alpha synucleinopathies and brain iron deposition.

In conclusion, MPAN should be considered with the onset of behavioral and cognitive deficits, extrapyramidal symptoms, and pyramidal signs even in patients presenting in the fourth decade of life. At 35 years of age, this is the oldest onset of MPAN reported, corroborating the link between p.T11M C19orf12 mutations and an older age of clinical disease onset in MPAN. This is the first report of a brain FDG-PET scan in a patient with MPAN, and it reveals asymmetric hypometabolism. Along with PD, dementia with Lewy bodies, multiple system atrophy, pure autonomic failure, some amyloidoses, some tauopathies, and PLAN, MPAN should be considered to be an alpha-synucleinopathy (Gregory et al., 2008; Jellinger, 2003; Li et al., 2013). Hopefully, the recognition and analysis of future cases of MPAN will help reveal the function of the C19orf12 gene product and clarify the pathogenesis of other alpha-synucleinopathies and NBIAs.

Acknowledgments

We thank the patient and his family for their contribution to this work.

References

Al-Semari A, Bohlega S. Autosomal-recessive syndrome with alopecia, hypogonadism, progressive extra-pyramidal disorder, white matter disease, sensory neural deafness, diabetes mellitus, and low IGF1. American Journal of Medical Genetics Part A. 2007; 143a:149–160. DOI: 10.1002/ajmg.a.31497 [PubMed: 17167799]

Amaral LLF, Gaddikeri S, Chapman PR, Roy R, Gaddikeri RS, Marussi VH, Bag AK. Neurodegeneration with brain iron accumulation: Clinicoradiological approach to diagnosis. Journal of Neuroimaging. 2015; 25:539–551. DOI: 10.1111/jon.12195 [PubMed: 25545045]

Aoki S, Okada Y, Nishimura K, Barkovich AJ, Kjos BO, Brasch RC, Norman D. Normal deposition of brain iron in childhood and adolescence: MR imaging at 1.5 T. Radiology. 1989; 172:381–385. DOI: 10.1148/radiology.172.2.2748819 [PubMed: 2748819]

Aoun M, Tiranti V. Mitochondria: A crossroads for lipid metabolism defect in neurodegeneration with brain iron accumulation diseases. The International Journal of Biochemistry & Cell Biology. 2015; 63:25–31. DOI: 10.1016/j.biocel.2015.01.018 [PubMed: 25668476]

Colombelli C, Aoun M, Tiranti V. Defective lipid metabolism in neurodegeneration with brain iron accumulation (NBIA) syndromes: Not only a matter of iron. Journal of Inherited Metabolic Disease. 2015; 38:123–136. DOI: 10.1007/s10545-014-9770-z [PubMed: 25300979]

Cossu G, Abbruzzese G, Matta G, Murgia D, Melis M, Ricchi V, … Forni GL. Efficacy and safety of deferiprone for the treatment of pantothenate kinase-associated neurodegeneration (PKAN) and neurodegeneration with brain iron accumulation (NBIA): Results from a four years follow-up. Parkinsonism & Related Disorders. 2014; 20:651–654. DOI: 10.1016/j.parkreldis.2014.03.002 [PubMed: 24661465]

del C Valdés Hernández M, Glatz A, Kiker AJ, Dickie DA, Aribisala BS, Royle NA, … Wardlaw JM. Differentiation of calcified regions and iron deposits in the ageing brain on conventional structural MR images. Journal of Magnetic Resonance Imaging. 2014; 40:324–333. DOI: 10.1002/jmri.24348 [PubMed: 24923620]

del C Valdés Hernández M, Maconick LC, Tan EMJ, Wardlaw JM. Identification of mineral deposits in the brain on radiological images: A systematic review. European Radiology. 2012; 22:2371–2381. DOI: 10.1007/s00330-012-2494-2 [PubMed: 22688125]

Deschauer M, Gaul C, Behrmann C, Prokisch H, Zierz S, Haack TB. C19orf12 mutations in neurodegeneration with brain iron accumulation mimicking juvenile amyotrophic lateral sclerosis. Journal of Neurology. 2012; 259:2434–2439. DOI: 10.1007/s00415-012-6521-7 [PubMed: 22584950]

Dezfouli MA, Alavi A, Rohani M, Rezvani M, Nekuie T, Klotzle B, … Elahi E. PANK2 and C19orf12 mutations are common causes of neurodegeneration with brain iron accumulation. Movement Disorders. 2013; 28:228–232. DOI: 10.1002/mds.25271 [PubMed: 23166001]

Dogu O, Krebs CE, Kaleagasi H, Demirtas Z, Oksuz N, Walker RH, Paisán-Ruiz C. Rapid disease progression in adult-onset mitochondrial membrane protein-associated neurodegeneration. Clinical Genetics. 2013; 84:350–355. DOI: 10.1111/cge.12079 [PubMed: 23278385]

Dusi S, Valletta L, Haack TB, Tsuchiya Y, Venco P, Pasqualato S, … Tiranti V. Exome sequence reveals mutations in CoA synthase as a cause of neurodegeneration with brain iron accumulation. The American Journal of Human Genetics. 2014; 94:11–22. DOI: 10.1016/j.ajhg.2013.11.008 [PubMed: 24360804]

Freeman K, Gregory A, Turner A, Blasco P, Hogarth P, Hayflick S. Intellectual and adaptive behaviour functioning in pantothenate kinase-associated neurodegeneration. Journal of Intellectual Disability Research. 2007; 51:417–426. DOI: 10.1111/j.1365-2788.2006.00889.x [PubMed: 17493025]

Gagliardi M, Annesi G, Lesca G, Broussolle E, Iannello G, Vaiti V, … Quattrone A. C19orf12 gene mutations in patients with neurodegeneration with brain iron accumulation. Parkinsonism & Related Disorders. 2015; 21:813–816. DOI: 10.1016/j.parkreldis.2015.04.009 [PubMed: 25962551]

Goldman JG, Eichenseer SR, Berry-Kravis E, Zimnowodzki S, Gregory A, Hogarth P, Hayflick SJ. Clinical features of neurodegeneration with brain iron accumulation due to a C19orf12 gene mutation. Movement Disorders. 2013; 28:1462–1463. DOI: 10.1002/mds.25410 [PubMed: 23494994]

Gregory, A., Hartig, M., Prokisch, H., Kmiec, T., Hogarth, P., Hayflick, SJ. Mitochondrial membrane protein-associated neurodegeneration. In: Pagon, RA.Adam, MP.Ardinger, HH.Wallace, SE.Amemiya, A.Bean, LJH., … Stephens, K., editors. Genegener(R). Seattle: University of Washington; 2014.

Gregory, A., Hayflick, S. Neurodegeneration with brain iron accumulation disorders overview. In: Pagon, RA.Adam, MP.Ardinger, HH.Wallace, SE.Amemiya, A.Bean, LJH., … Stephens, K., editors. GeneReviews(R). Seattle: University of Washington; 2014.

Gregory A, Westaway SK, Holm IE, Kotzbauer PT, Hogarth P, Sonek S, … Hayflick SJ. Neurodegeneration associated with genetic defects in phospholipase A2. Neurology. 2008; 71:1402–1409. DOI: 10.1212/01.wnl.0000327094.67726.28 [PubMed: 18799783]

Haack TB, Hogarth P, Kruer MC, Gregory A, Wieland T, Schwarzmayr T, … Hayflick SJ. Exome sequencing reveals de novo WDR45 mutations causing a phenotypically distinct, X-linked dominant form of NBIA. The American Journal of Human Genetics. 2012; 91:1144–1149. DOI: 10.1016/j.ajhg.2012.10.019 [PubMed: 23176820]

Hartig M, Prokisch H, Meitinger T, Klopstock T. Mitochondrial membrane protein-associated neurodegeneration (MPAN). International Review of Neurobiology. 2013; 110:73–84. DOI: 10.1016/b978-0-12-410502-7.00004-1 [PubMed: 24209434]

Hartig MB, Iuso A, Haack T, Kmiec T, Jurkiewicz E, Heim K, … Prokisch H. Absence of an orphan mitochondrial protein, c19orf12, causes a distinct clinical subtype of neurodegeneration with brain iron accumulation. The American Journal of Human Genetics. 2011; 89:543–550. DOI: 10.1016/j.ajhg.2011.09.007 [PubMed: 21981780]

Hayflick SJ. Defective pantothenate metabolism and neurodegeneration. Biochemical Society Transactions. 2014; 42:1063–1068. DOI: 10.1042/bst20140098 [PubMed: 25110003]

Hayflick SJ, Hartman M, Coryell J, Gitschier J, Rowley H. Brain MRI in neurodegeneration with brain iron accumulation with and without PANK2 mutations. AJNR. American Journal of Neuroradiology. 2006; 27:1230–1233. [PubMed: 16775270]

Hegde AN, Mohan S, Lath N, Lim CC. Differential diagnosis for bilateral abnormalities of the basal ganglia and thalamus. Radiographics. 2011; 31:5–30. DOI: 10.1148/rg.311105041 [PubMed: 21257930]

Hogarth P, Gregory A, Kruer MC, Sanford L, Wagoner W, Natowicz MR, … Hayflick SJ. New NBIA subtype: Genetic, clinical, pathologic, and radiographic features of MPAN. Neurology. 2013; 80:268–275. DOI: 10.1212/WNL.0b013e31827e07be [PubMed: 23269600]

International Huntington Association and the World Federation of Neurology Research Group on Huntington's Chorea. Guidelines for the molecular genetics predictive test in Huntington's disease. Journal of Medical Genetics. 1994; 31:555–559. [PubMed: 7966192]

Jellinger KA. Neuropathological spectrum of synucleinopathies. Movement Disorders. 2003; 18:S2–S12. DOI: 10.1002/mds.10557 [PubMed: 14502650]

Karkheiran S, Shahidi GA, Walker RH, Paisan-Ruiz C. PLA2G6-associated dystonia-parkinsonism: Case report and literature review. Tremor and Other Hyperkinetic Movements (New York, N.Y.). 2015; 5:317.doi: 10.7916/d84q7t4w

Keogh MJ, Jonas P, Coulthard A, Chinnery PF, Burn J. Neuroferritinopathy: A new inborn error of iron metabolism. Neurogenetics. 2012; 13:93–96. DOI: 10.1007/s10048-011-0310-9 [PubMed: 22278127]

Kleffner I, Wessling C, Gess B, Korsukewitz C, Allkemper T, Schirmacher A, … Husstedt IW. Behr syndrome with homozygous C19ORF12 mutation. Journal of the Neurological Sciences. 2015; 357:115–118. DOI: 10.1016/j.jns.2015.07.009 [PubMed: 26187298]

Kurian MA, Hayflick SJ. Pantothenate kinase-associated neurodegeneration (PKAN) and PLA2G6-associated neurodegeneration (PLAN): Review of two major neurodegeneration with brain iron accumulation (NBIA) phenotypes. International Review of Neurobiology. 2013; 110:49–71. DOI: 10.1016/b978-0-12-410502-7.00003-x [PubMed: 24209433]

Landoure G, Zhu PP, Lourenco CM, Johnson JO, Toro C, Bricceno KV, … Burnett BG. Hereditary spastic paraplegia type 43 (SPG43) is caused by mutation in C19orf12. Human Mutation. 2013; 34:1357–1360. DOI: 10.1002/humu.22378 [PubMed: 23857908]

Lehn A, Boyle R, Brown H, Airey C, Mellick G. Neuroferritinopathy. Parkinsonism & Related Disorders. 2012; 18:909–915. DOI: 10.1016/j.parkreldis.2012.06.021 [PubMed: 22818529]

Levi S, Finazzi D. Neurodegeneration with brain iron accumulation: Update on pathogenic mechanisms. Frontiers in Pharmacology. 2014; 5:99.doi: 10.3389/fphar.2014.00099 [PubMed: 24847269]

Levine IM, Estes JW, Looney JM. Hereditary neurological disease with acanthocytosis. A new syndrome. Archives of Neurology. 1968; 19:403–409. DOI: 10.1001/archneur.1968.00480040069007 [PubMed: 5677189]

Li A, Paudel R, Johnson R, Courtney R, Lees AJ, Holton JL, … Houlden H. Pantothenate kinase-associated neurodegeneration is not a synucleinopathy. Neuropathology and Applied Neurobiology. 2013; 39:121–131. DOI: 10.1111/j.1365-2990.2012.01269.x [PubMed: 22416811]

Mahoney R, Selway R, Lin JP. Cognitive functioning in children with pantothenate-kinase-associated neurodegeneration undergoing deep brain stimulation. Developmental Medicine & Child Neurology. 2011; 53:275–279. DOI: 10.1111/j.1469-8749.2010.03815.x [PubMed: 21166667]

Margolis, RL. Huntington disease-like 2. In: Pagon, RA.Adam, MP.Ardinger, HH.Wallace, SE.Amemiya, A.Bean, LJH., … Stephens, K., editors. GeneReviews(R). Seattle: University of Washington; 2012.

Margolis RL, O'Hearn E, Rosenblatt A, Willour V, Holmes SE, Franz ML, … Ross CA. A disorder similar to Huntington's disease is associated with a novel CAG repeat expansion. Annals of Neurology. 2001; 50:373–380. DOI: 10.1002/ana.1312

McNeill A, Pandolfo M, Kuhn J, Shang H, Miyajima H. The neurological presentation of ceruloplasmin gene mutations. European Neurology. 2008; 60:200–205. DOI: 10.1159/000148691 [PubMed: 18667828]

Meyer E, Kurian MA, Hayflick SJ. Neurodegeneration with brain iron accumulation: Genetic diversity and pathophysiological mechanisms. Annual Review of Genomics and Human Genetics. 2015; 16:257–279. DOI: 10.1146/annurev-genom-090314-025011

Points to consider in the clinical application of genomic sequencing. Retrieved from https://www.acmg.net/StaticContent/PPG/Clinical_Application_of_Genomic_Sequencing.pdf

Rabbani B, Tekin M, Mahdieh N. The promise of whole-exome sequencing in medical genetics. Journal of Human Genetics. 2014; 59:5–15. DOI: 10.1038/jhg.2013.114 [PubMed: 24196381]

Schenck JF. Imaging of brain iron by magnetic resonance: T2 relaxation at different field strengths. Journal of the Neurological Sciences. 1995; 134:10–18. DOI: 10.1016/0022-510X(95)00203-E [PubMed: 8847539]

Schneider SA, Bhatia KP. Syndromes of neurodegeneration with brain iron accumulation. Seminars in Pediatric Neurology. 2012; 19:57–66. DOI: 10.1016/j.spen.2012.03.005 [PubMed: 22704258]

Schneider SA, Dusek P, Hardy J, Westenberger A, Jankovic J, Bhatia KP. Genetics and pathophysiology of neurodegeneration with brain iron accumulation (NBIA). Current Neuropharmacology. 2013; 11:59–79. DOI: 10.2174/157015913804999469 [PubMed: 23814539]

Schrag A, Ben-Shlomo Y, Brown R, Marsden CD, Quinn N. Young-onset Parkinson's disease revisited–clinical features, natural history, and mortality. Movement Disorders. 1998; 13:885–894. DOI: 10.1002/mds.870130605 [PubMed: 9827611]

Schulte EC, Claussen MC, Jochim A, Haack T, Hartig M, Hempel M, … Ilg R. Mitochondrial membrane protein associated neurodegenration: A novel variant of neurodegeneration with brain iron accumulation. Movement Disorders. 2013; 28:224–227. DOI: 10.1002/mds.25256 [PubMed: 23436634]

Skowronska M, Kmiec T, Kurkowska-Jastrzębska I, Czlonkowska A. Eye of the tiger sign in a 23 year patient with mitochondrial membrane protein associated neurodegeneration. Journal of the Neurological Sciences. 2015; 352:110–111. DOI: 10.1016/j.jns.2015.03.019 [PubMed: 25819119]

Stevenson VL, Hardie RJ. Acanthocytosis and neurological disorders. Journal of Neurology. 2001; 248:87–94. DOI: 10.1007/s004150170241 [PubMed: 11284140]

Venco P, Bonora M, Giorgi C, Papaleo E, Iuso A, Prokisch H, … Tiranti V. Mutations of C19orf12, coding for a transmembrane glycine zipper containing mitochondrial protein, cause mis-localization of the protein, inability to respond to oxidative stress and increased mitochondrial Ca2+ Frontiers in Genetics. 2015; 6:185.doi: 10.3389/fgene.2015.00185 [PubMed: 26136767]

Williams DR, Hadeed A, al-Din ASN, Wreikat AL, Lees AJ. Kufor Rakeb disease: Autosomal recessive, levodopa-responsive parkinsonism with pyramidal degeneration, supranuclear gaze palsy, and dementia. Movement Disorders. 2005; 20:1264–1271. DOI: 10.1002/mds.20511 [PubMed: 15986421]

Yonekawa M, Okabe T, Asamoto Y, Ohta M. A case of hereditary ceruloplasmin deficiency with iron deposition in the brain associated with chorea, dementia, diabetes mellitus and retinal pigmentation: Administration of fresh-frozen human plasma. European Neurology. 1999; 42:157–162. DOI: 10.1159/000008091 [PubMed: 10529542]

Zorzi G, Zibordi F, Chiapparini L, Bertini E, Russo L, Piga A, Nardocci N. Iron-related MRI images in patients with pantothenate kinase-associated neurodegeneration (PKAN) treated with deferiprone: Results of a phase II pilot trial. Movement Disorders. 2011; 26:1755–1759. DOI: 10.1002/mds.23751

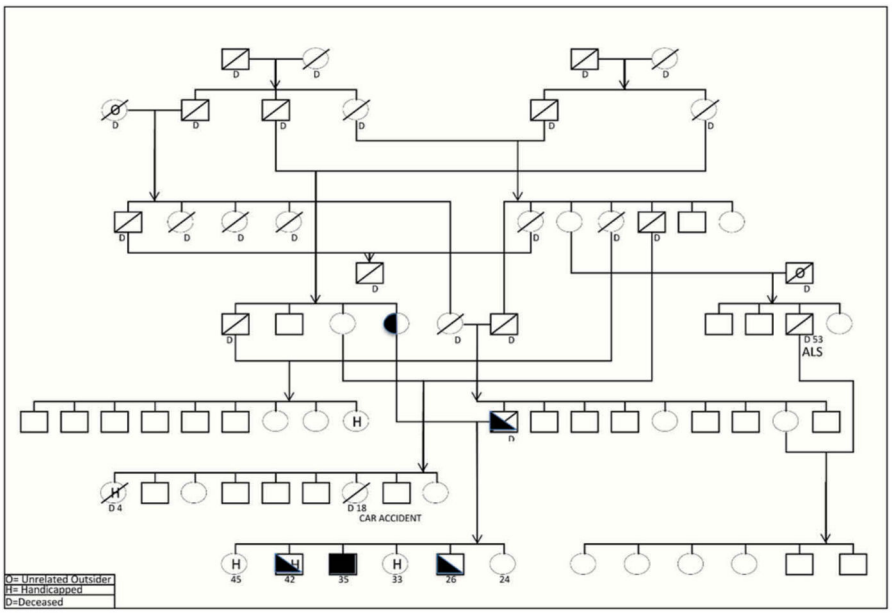

Figure 1.

Pedigree provided by the patient's uncle demonstrating the consanguinity of the patient's (proband's) parents.

The proband, a homozygote for the C19orf12 mutation, is depicted by a black square at the bottom. Heterozygotes are half shaded.

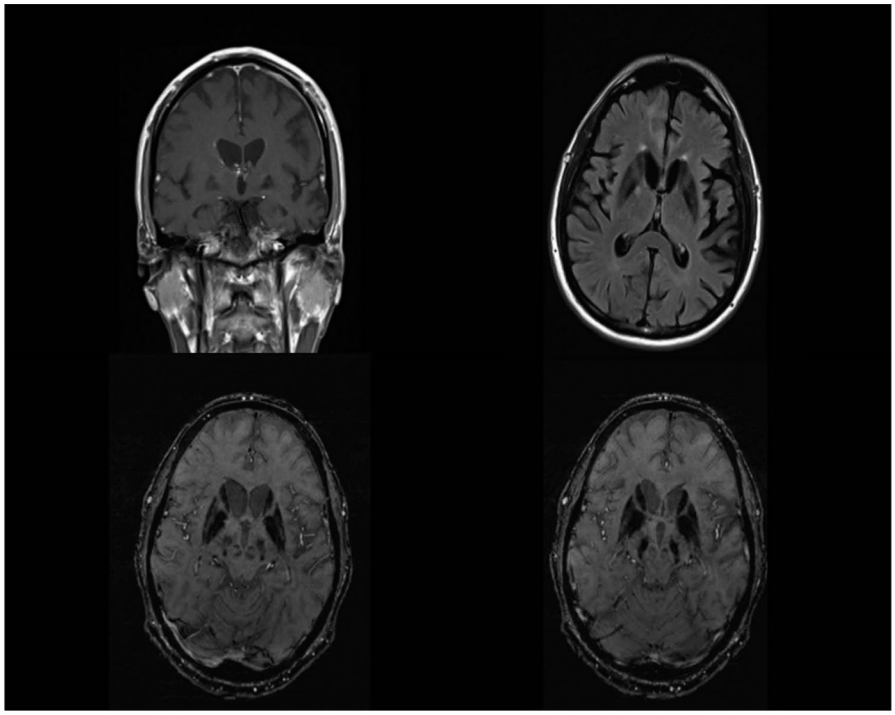

Figure 2.

Top left: 3T MRI T1 coronal image with contrast showing bifrontal parenchymal volume loss, asymmetric parenchymal volume loss of the temporal lobes, and hypointensity of the globi pallidi. Top right: 3T MRI FLAIR axial image showing hypointensity of the globi pallidi and putamina, mild periventricular white matter hyperintensities, and left greater than right temporoparietal parenchymal volume loss. Bottom left: 3T MRI susceptibility weighted image (SWI) showing hypointensity of the globi pallidi, caudate heads, and putamina and relatively hyperintense streaking of the medullary laminae. Bottom right: 3T MRI SWI showing hypointensity of the substantiae nigrae as well as the globi pallidi, caudate heads, and putamina.

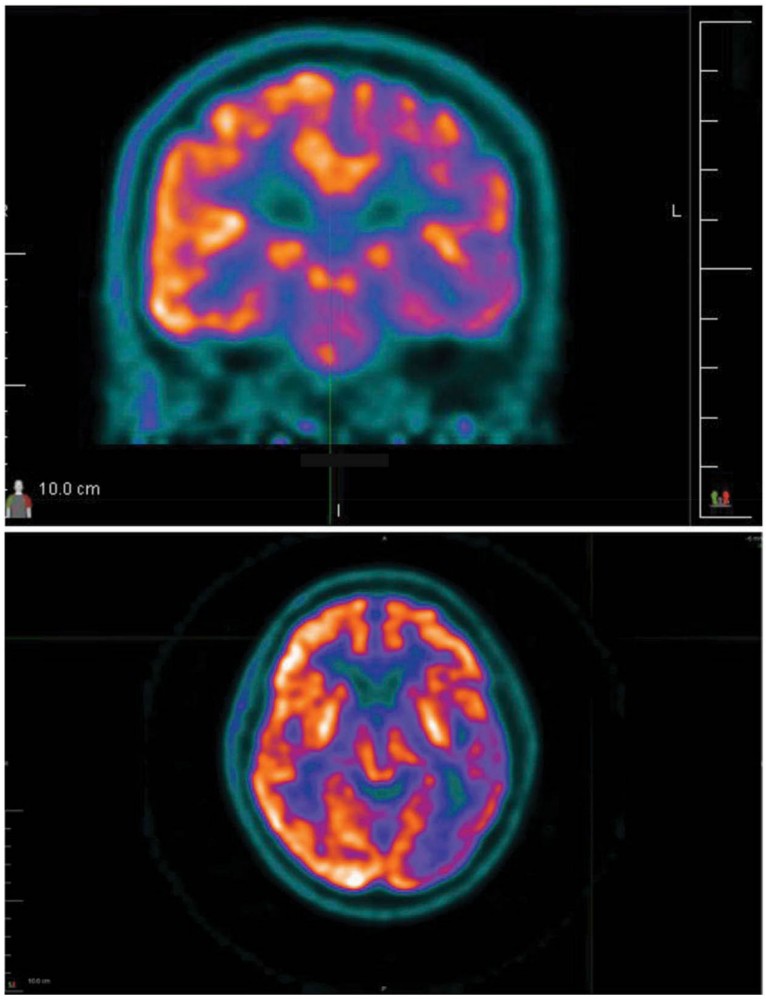

Figure 3.

Top: FDG-PET axial image showing relative hypoperfusion of the left temporal, parietal, occipital, and insular frontal cortices. Bottom: FDG-PET coronal image showing relative hypoperfusion of the left frontal and temporal cortices.

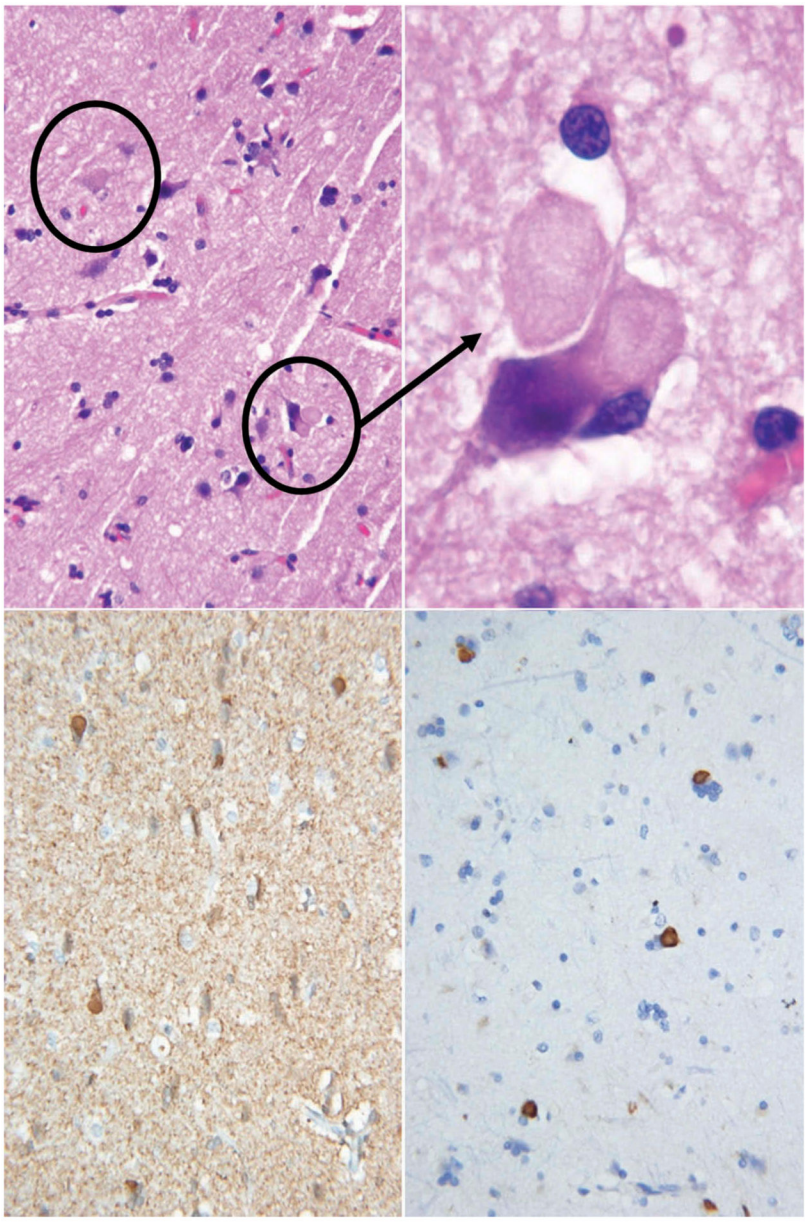

Figure 4.

Top left: Hematoxylin and eosin stain of cortex showing spherical neuronal intracytoplasmic inclusions resembling Lewy bodies in the top circle and similar extra-neuronal inclusions in the bottom circle. Top right: Hematoxylin and eosin stain of cortex with a higher magnification view of the extra-neuronal inclusions that resemble extra-neuronal Lewy bodies. Bottom left: Alpha synuclein immunohistochemistry staining of the intracytoplasmic inclusions. Bottom right: Ubiquitin-binding protein p62 immunohistochemistry staining of the intracytoplasmic inclusions.

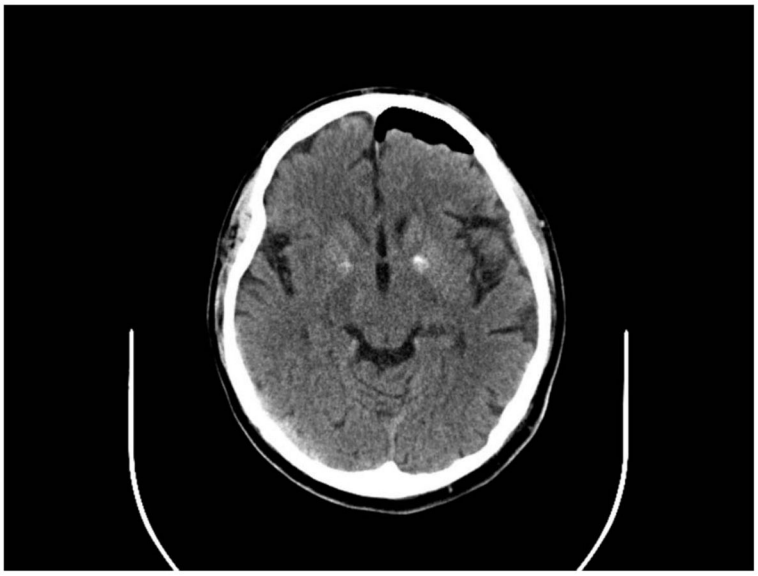

Figure 5.
CT axial image showing bilateral hyperdensities in the globi pallidi and pneumocephaly from a left frontal brain biopsy.

Table 1

Information on the 10 known types of NBIA (Al-Semari & Bohlega, 2007; Dusi et al., 2014; Gregory & Hayflick, 2014; Haack et al., 2012; Kurian & Hayflick, 2013; Schneider & Bhatia, 2012).

NBIA type	Mutation	Onset	Symptoms	Pearls
PKAN	PANK2	Early – 3 years old Atypical teens and 20s	Early-spastic paraparesis, dystonia, rigidity, pigmentary retinopathy, step-wise decline to inability to walk over 10–15 years Atypical-dysarthria, palilalia, slower progression	35–50% of NBIA Eye of the tiger
Phospholipase A2 group VI associated neurodegeneration (PLAN) (PARK14)	PLA2G6	Infantile – <3 years Atypical teens PRDP – age 4–30	Infantile-ataxia, spastic tetraparesis, death by age 10 Atypical-ataxia, social communication deficits, impulsivity, dystonia PRDP – dysarthria, dystonia, Parkinsonism, dopamine-induced dyskinesia	20% of NBIA Cerebellar parenchymal volume loss and gliosis and secondary thinning of the posterior corpus callosum Claval hypertrophy Only half have elevated brain iron on MRI
MPAN	C19orf12	3–35 years old (mean of 10)	Spasticity > dystonia, optic parenchymal volume loss, Parkinsonism, nearly universal progression to dementia, early urinary incontinence, motor axonal peripheral neuropathy	T2 hyperintense streaking of medullary lamina in some
FAHN	FA2H	Childhood or adolescence	Spasticity, dystonia, optic parenchymal volume loss, supranuclear gaze palsy	Associated with leukodystrophy
Kufor–Rakeb syndrome (PARK9)	ATPase type 13A2	Usually adolescence but into 30s	Pyramidal signs, levodopa responsive Parkinsonism with early dopamine-induced dyskinesia	Not all have elevated brain iron visible on MRI
BPAN	WDR45	Early childhood	Global delay in early childhood with development of Parkinsonism, dystonia, and dementia in adulthood	X-linked dominant

NBIA type	Mutation	Onset	Symptoms	Pearls
CoPAN	CoASY	2–3 years old	Toe walking and by grade school dystonia; by age 20, tics, dementia, and inability to walk, motor neuropathy	CoASY catalyzes the final two of three steps in the synthesis of coenzyme A from pantothenate (PANK2 catalyzes the first)
Neuroferritinopathy	FTL1	Adulthood (mean of 39)	Asymmetric chorea or dystonia, low ferritin	Autosomal dominant Cortical iron on susceptibility weighted MRI
Aceruloplasminemia	Ceruloplasmin	16–71 (mean of 51)	Dementia, retinal degeneration, diabetes, iron deficiency anemia, ceruloplasmin undetectable	Iron seen in the basal ganglia, thalamus, cerebellum, cortex, pancreas, and liver
Woodhouse–Sakati syndrome	DCAF17	Evident at puberty	Alopecia, hypogonadism (small testes or streak ovaries), sensorineural deafness, low insulin-like growth factor 1, chorea, dystonia, scoliosis	White matter changes

PKAN: Pantothenate kinase-associated neurodegeneration; PANK: pantothenate kinase; PLA2G6: phospholipase A2 group VI; PRDP: PLA2G6-related dystonia-Parkinsonism; MPAN: mitochondrial membrane protein associated neurodegeneration; C19orf12: chromosome 19 open reading frame 12; FAHN: fatty acid hydroxylase-associated neurodegeneration; FA2H: fatty acid 2 hydroxylase; BPAN: beta propeller associated neurodegeneration; WDR45: WD repeat 45; CoPAN: coenzyme A synthase protein associated neurodegeneration; CoASY: coenzyme A synthase; FTL: ferritin light chain; DCAF: DDB1- and CUL4-associated factor.